Received: 21 September 2017 | Revised: 11 January 2018 | Accepted: 27 May 2018

DOI: 10.4218/etrij.2017-0204

ORIGINAL ARTICLE

WILEY ETRI Journal

Performance analysis of large-scale MIMO system for wireless backhaul network

Seokki Kim | **Seungkwon Baek**

Hyper-connected Communication Research Laboratory, Electronics and Telecommunications Research Institute, Daejeon, Rep. of Korea.

Correspondence
Seokki Kim, Hyper-connected Communication Research Laboratory, Electronics and Telecommunications Research Institute, Daejeon, Rep. of Korea.
Email: kimsk0729@etri.re.kr

Funding information
Ministry of Science, ICT and Future Planning, Grant/Award Number: 2014-0-00282.

In this paper, we present a performance analysis of large-scale multi-input multi-output (MIMO) systems for wireless backhaul networks. We focus on fully connected N nodes in a wireless meshed and multi-hop network topology. We also consider a large number of antennas at both the receiver and transmitter. We investigate the transmission schemes to support fully connected N nodes for half-duplex and full-duplex transmission, analyze the achievable ergodic sum rate among N nodes, and propose a closed-form expression of the achievable ergodic sum rate for each scheme. Furthermore, we present numerical evaluation results and compare the resuts with closed-form expressions.

KEYWORDS
full duplex, large-scale MIMO, massive MIMO, mesh topology, wireless backhaul network

1 | INTRODUCTION

A number of requirements have been proposed to enable fifth-generation (5G) mobile systems, which is the next major phase of telecommunications standards, to realize the 5G vision for user experience and system performance [1,2]. The most important requirement is to support an extremely high data rate as mobile data traffic continues to rapidly increase owing to the increased availability of mobile smart devices and the development of different application services. To support the high mobile data traffic, researchers are currently considering broadband transmission using millimeter-wave (mmWave) frequency bands, high spectrum efficiency exploiting multi-input multi-output (MIMO) and full-duplex (FD) transmission, and network densification using a large number of access points such as small cells, relays, or distributed radio units as key enabling technologies [3]. With the increase of data traffic in mobile access networks, it is also important to increase the backhaul capacity, which provides a connection with a core network. Unfortunately, the use of optical fiber as in existing backhaul networks results in implementation cost problems.

Recently, many works have focused on wireless backhaul using the mmWave frequency band and large-scale MIMO technology, with the aim of realizing cost-effectiveness, high throughput, and low latency. References [4] and [5] present a system scenario of cellular networks with a mmWave backhaul link and an application of large-scale MIMO technology for wireless backhaul links, respectively. The benefits and challenges of a large-scale MIMO-based wireless backhaul in heterogeneous networks are discussed in [6]. Reference [7] derives theoretical upper and lower bounds on capacity, and studies the scalability of wireless backhaul networks that use the mmWave frequency band and large-scale MIMO.

There has also been research focusing on the utilization of FD technology for the wireless backhaul. Reference [8] introduces FD technology as a solution to enhance the throughput for wireless backhaul networks, such as the FD relay in mmWave backhaul links proposed in [9] and self-backhauling heterogeneous networks using FD capability, as proposed in [10]. Reference [11] addresses self-interference (SI) mitigation, which is an important issue related to FD technology.

Moreover, it is necessary to support meshed and multi-hop network topologies in order to overcome severe

conditions that affect the mmWave frequency band such as signal blockages or large attenuation, and to improve the reliability and efficiency in the wireless backhaul network. Reference [12] demonstrates the performance gain of the mesh topology compared with the star topology.

However, existing works related to wireless backhaul with mmWave and large-scale MIMO address primarily backhaul links for small cells in heterogeneous networks, and do not consider in detail the effects of interference, especially SI and SI cancelation (SIC), depending on different transmission schemes with respect to the use of FD technology. Therefore, it is necessary to study transmission schemes considering duplex transmission, and to analyze the performance considering the effects of interference to support general mesh topology for wireless backhaul networks with mmWave and large-scale MIMO.

We consider a general mesh topology as a simple connection of multiple groups with fully connected nodes, as illustrated in Figure 1. If FD technology is not employed, orthogonal resources may have to be allocated in order for the nodes in the group to avoid SI, which results in a decrease in the spectral efficiency. If FD technology is employed, interference increases proportionally with the number of nodes in the group, which results in a decrease in the quality of the received signal. Therefore, in this paper, we focus on fully connected N nodes because the number of nodes that are fully connected is the dominant parameter influencing the performance.

We consider a large number of antennas at both the receiver and transmitter. For radio transmission, the main challenge among fully connected N nodes is interference, which degrades the spectrum efficiency and limits link connectivity. To address the issue, we also consider large-scale MIMO and FD.

The large-scale MIMO presented in [13] is an extreme version of multi-user MIMO. For a base station with a large number of antennas and a mobile station with a small number of antennas, transmission and reception techniques such as maximum ratio transmission (MRT), zero-forcing (ZF), maximum ratio combining (MRC), and minimum mean square error (MMSE) were studied in [13–15]. The use of FD transmission is able to theoretically double the spectrum efficiency between two nodes. There have been many studies on the SIC technique because it is an essential approach to the theoretical bound on capacity [16–18].

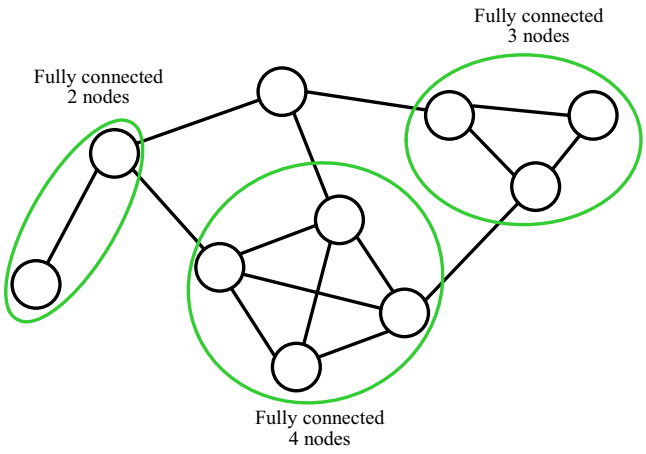

FIGURE 1 Fully connected N nodes in wireless meshed and multi-hop network topology

The main contributions of this paper are as follows. First, we investigate the transmission schemes to support fully connected N nodes for half-duplex (HD) and FD transmission. Then, we analyze the achievable ergodic sum rate among N nodes for each scheme. Finally, we propose closed-form expressions of an achievable ergodic sum rate with approximations.

Throughout this paper, $A := B$ denotes that by definition, A equals to B, a boldface uppercase denotes a matrix, a boldface lowercase denotes a vector, $[\cdot]^{\mathrm{H}}$ denotes the conjugate transpose, $\mathrm{E}[\cdot]$ denotes the expectation, $|\cdot|$ denotes the absolute value for a scalar or the number of elements for a set, $\|\cdot\|$ denotes the Frobenius norm, $\lfloor\cdot\rfloor$ and $\lceil\cdot\rceil$ denote the floor and ceiling, respectively, ${}_n\mathrm{C}_k$ denotes the number of k combinations from a given set of n elements, and $\mathbf{I}$ denotes an identity matrix.

Furthermore, we attach specific equations, namely, (1) to (5), (12) to (16), and (30) to (34) at the end of this paper owing to space constraints and readability.

2 | SYSTEM MODEL

2.1 | Transmission schemes for fully connected N nodes

To support fully connected links among N nodes equipped with a large number of antennas and operating in HD, we first consider simple transmission schemes that exploit massive MIMO in cellular networks; that is, transmission over a broadcast channel (BC) such as downlink (DL), or transmission over a multiple-access channel (MAC) such as uplink (UL). We define these as a BC-based scheme and MAC-based scheme, respectively. However, because a large number of antennas are available at both the receiver and transmitter, we can anticipate the throughput enhancement through the transmission over a K-user interference channel (K-User IC). We define this as a K-UserIC-based scheme. Furthermore, we can more efficiently support fully connected N nodes by exploiting FD. We classify the transmission schemes based on FD into two categories considering the spatial separation between the nodes, transmission based on in-band full-duplex (IBFD) and transmission based on space-division duplex (SDD). We define the former as an IBFD-based scheme and the latter as an SDD-based scheme. For the IBFD-based scheme, a bidirectional

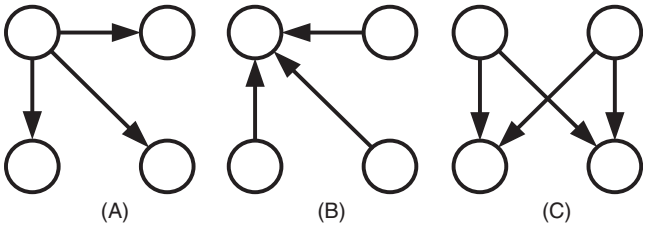

FIGURE 2 Transmission schemes based on HD to support fully connected N nodes: (A) BC-based scheme, (B) MAC-based scheme, and (C) K-UserIC-based scheme

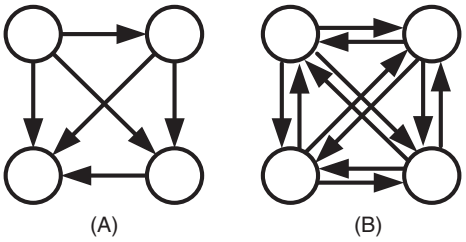

FIGURE 3 Transmission schemes based on FD to support fully connected N nodes: (A) SDD-based scheme and (B) IBFD-based scheme

link is permitted between any pair of nodes; for an SDD-based scheme, only a unidirectional link is permitted.

Consider a wireless system, as illustrated in Figure 2, where the fully connected N nodes are equipped with M_T and M_R antennas for transmission and reception, respectively. For node index $i = 1, 2, \ldots, N$ and $j = 1, 2, \ldots, N$, let $\mathbf{x}_{ij}$, $\mathbf{H}_{ij}$, and $\mathbf{n}_j$ be the transmitted signal vectors from nodes i to j, MIMO channel matrix from node i to j, and noise vector of node j. Furthermore, let $\mathbf{f}_{ij}$ and $\mathbf{g}_{ij}$, respectively, be the precoding vector at the transmitter and combining vector at the receiver for the desired signal from nodes i to j. We assume that the channel $\mathbf{H}_{ij}$, where i is not equal to j, is flat MIMO Rayleigh fading, and all channels between any pair of nodes are independent and identically distributed (i.i.d). If i is equal to j, then $\mathbf{H}_{ij}$ denotes an SI channel. We also assume that the entries of noise vector $\mathbf{n}_{ij}$ are zero-mean circular symmetry complex Gaussian (ZMCSCG) distribution with a variance of σ^2. Finally, the transmitted signal $\mathbf{x}_{ij}$ satisfies $\mathrm{E}[\mathbf{x}_{ij}\mathbf{x}_{ij}^{\mathrm{H}}] = \mathbf{I}$, and the transmit power of each node is limited by P.

For the BC-based scheme illustrated in Figure 2A, one node transmits the signal to $(N - 1)$ nodes simultaneously. The wireless resource is partitioned into N, and is alternately occupied by all nodes. The received signal at node j^* is expressed by (1) (see end of paper for (1) to (5)). For the MAC-based scheme illustrated in Figure 2B, $(N - 1)$ nodes transmit the signal to one node simultaneously. The wireless resource is partitioned into N, and is alternately occupied by all nodes. The received signal at node j^* is expressed by (2). For the K-UserIC-based scheme illustrated in Figure 2C, K nodes transmit the signal to $(N - K)$ nodes simultaneously. The wireless resource is partitioned into ${}_N\mathrm{C}_K$, and is occupied by all K combinations of the nodes in rotation. The received signal at node j^* is expressed by (3), where K denotes the number of transmit nodes, which results in $(N - K)$ receive nodes. For the SDD-based scheme illustrated in Figure 3A, for any pair of nodes, one node transmits the signal to another. The wireless resource is partitioned into two and the partitioned resources are used for bidirectional communication between any pair of nodes. The received signal at node j^* is expressed by (4), where $S_T(j)$ and $S_R(i)$ denote the sets where the elements are the index of the transmit nodes whose receiver is node j and the index of the receive nodes whose transmitter is node i, respectively. For the IBFD-based scheme illustrated in Figure 3B, N nodes transmit the signal to $(N - 1)$ nodes simultaneously. The wireless resource does not have to be partitioned. The received signal at node j^* is expressed by (5).

From (1) to (5), the interference is divided by the BC interference term, MAC interference term, co-channel interference term, and SI term.

Although the number of transmit nodes for the K-UserIC-based scheme, K, and the sets of transmit and receive nodes for the SDD-based scheme, $S_T(j)$ and $S_R(i)$, have an influence on performance, in this paper, we do not address the optimization of the parameters. Rather, for simplicity, for the K-UserIC-based scheme, we consider $(N/2)$ as the K value, and for the SDD-based scheme, we consider a randomly selected link direction between a pair of nodes.

If the influence of interference can be ignored, for the BC and MAC-based schemes, the transmission degree-of-freedom (DoF) among fully connected N nodes is $(N - 1)$. For the K-UserIC-based scheme, the DoF is $K(N - K)$, which is maximized when K is $(N/2)$. For the SDD-based scheme and IBFD, the DoF is $(N(N - 1)/2)$ and $N(N - 1)$, respectively. Thus, for a large N, the DoF of the K-UserIC-based scheme is improved $(N/4)$ times compared to the BC and MAC-based schemes. This is proportional to the number of nodes. However, the DoF of the SDD-based scheme and IBFD-based scheme is improved two and four times, respectively, compared to the K-UserIC-based scheme, regardless of the number of nodes.

For the transmission schemes based on HD, that is, the BC, MAC, and K-UserIC-based schemes, there may be a link connection constraint due to SI. Furthermore, because the number of partitioned resources depends on the number of fully connected nodes, resource scheduling must change based on N. For the transmission scheme based on FD, that is, the SDD- or IBFD-based schemes, the number of partitioned resources is independent of N, that is, two partitioned resources for the SDD-based scheme and no resource partitioning for the IBFD-based scheme. However, SIC is essential for the transmission schemes based on FD.

For the SDD-based scheme, nodes with and without SIC capability can coexist because SIC capability is not a

requirement for all nodes. Furthermore, the interference environment is favorable compared to the IBFD-based scheme.

2.2 | Maximal-ratio transmission and combining

In this paper, we do not consider spatial multiplexing MIMO between a pair of nodes because of the high directivity and insufficient rank of the MIMO channel in the mmWave frequency band. Diversity or array gain is more beneficial compared to spatial multiplexing in order to overcome the large attenuation of the transmit power in the mmWave frequency band. Furthermore, we consider the MRT and MRC schemes for the transmitter and receiver, respectively, because of their implementation simplicity, that is, the lack of requirement for a matrix inverse operation compared to the ZF or MMSE schemes.

We assume that transmit and receive channel-state information is available to the transmitter and receiver nodes, respectively, without error. To maximize the received signal power, precoding vector $\mathbf{f}_{ij}$ for MRT and combining vector $\mathbf{g}_{ij}$ for MRC between the transmit node i and receive node j are given by $\mathbf{f}_{ij} = \mathbf{v}_{ij,1}$ and $\mathbf{g}_{ij} = \mathbf{u}_{ij,1}{}^{\mathrm{H}}$, respectively. $\mathbf{u}_{ij,k}$ and $\mathbf{v}_{ij,k}$ are the k-th column of $\mathbf{U}_{ij}$ and $\mathbf{V}_{ij}$ obtained by singular value decomposition (SVD) of channel $\mathbf{H}_{ij}$ as $\mathbf{H}_{ij} = \mathbf{U}_{ij}\mathbf{\Sigma}_{ij}\mathbf{V}_{ij}{}^{\mathrm{H}}$, where $\mathbf{\Sigma}_{ij}$ is the rectangular diagonal matrix for which entries are the singular values in descending order. Thus, $\mathbf{u}_{ij,1}$ and $\mathbf{v}_{ij,1}$ are, respectively, the left and right singular vectors corresponding to the maximum singular value, and both $\|\mathbf{f}_{ij}\|^2$ and $\|\mathbf{g}_{ij}\|^2$ are equal to one.

2.3 | Self-interference and cancellation

SIC is an essential capability that supports FD operation because the SI power is significant compared to the desired signal. Many studies have focused on SIC. In general, SIC techniques are classified into propagation-domain interference suppression (PDIS) and analog and digital interference cancellation (ADIC) according to the cancellation domain.

Using the channel estimation error model of [19], considering the SI channel estimation error, SI channel $\mathbf{H}_{j^*j^*}$ is expressed by $\mathbf{H}_{j^*j^*} = (\hat{\mathbf{H}}_{j^*j^*} + \sqrt{e}\tilde{\mathbf{H}}_{j^*j^*})$, where $\hat{\mathbf{H}}_{j^*j^*}$, e, and $\tilde{\mathbf{H}}_{j^*j^*}$ denote the estimated SI channel, mean square error of the estimation, and ZMCSCG noise with unit variance, respectively. Thus, using the results of [20] and [21], the received signal after the completion of PDIS and ADIC at the receive node j^* with one SI link owing to node j is expressed by

$$\mathbf{y}'_{j^*} = \sqrt{P}\mathbf{H}_{i^*j^*}\mathbf{f}_{i^*j^*}\mathbf{x}_{i^*j^*} + \sqrt{\kappa P e}\tilde{\mathbf{H}}_{j^*j^*}\mathbf{f}_{j^*j}\mathbf{x}_{j^*j} + \mathbf{n}_j, \quad (6)$$

where κ denotes the SIC coefficient of PDIS. Although there is a difference in the received signal expression according to the SIC type, for simplicity, we used (6) as the SIC model regardless of the cancellation type. Furthermore, we define the overall SIC coefficient χ as $\chi := \kappa e$.

3 | PERFORMANCE ANALYSIS

3.1 | Achievable ergodic sum rate

We derived the achievable rate using the Shannon formula, $\log_2(1 + \mathrm{SINR})$, where SINR is defined as $\mathrm{SINR} := P_{\mathrm{S}}/(P_{\mathrm{I}} + P_{\mathrm{N}})$. P_{S}, P_{I}, and P_{N} denote the desired signal power, interference power, and noise power at the receiver, respectively. Thus, from (1), (2), (3), (4), and (5), after completion of SIC and MRC, that is, $\mathbf{g}_{i^*j^*}\mathbf{y}'_{j^*}$, the achievable ergodic sum rate for BC-based, MAC-based, K-UserIC-based, SDD-based, and IBFD-based schemes are, respectively, expressed by

$$\bar{\eta}_{\mathrm{sum}} = \mathrm{E}\left[\sum_{j^*\neq i^*}\log_2\left(1+\gamma_{i^*j^*,\mathrm{BC}}\right)\right], \quad (7)$$

$$\bar{\eta}_{\mathrm{sum}} = \mathrm{E}\left[\sum_{i^*\neq j^*}\log_2\left(1+\gamma_{i^*j^*,\mathrm{MAC}}\right)\right], \quad (8)$$

$$\bar{\eta}_{\mathrm{sum}} = \mathrm{E}\left[\sum_{i^*\leq K}\sum_{j^*>K}\log_2\left(1+\gamma_{i^*j^*,K\text{-UserIC}}\right)\right], \quad (9)$$

$$\bar{\eta}_{\mathrm{sum}} = \mathrm{E}\left[\sum_{i^*}\sum_{j^*\in S_{\mathrm{R}}(i^*)}\log_2\left(1+\gamma_{i^*j^*,\mathrm{SDD}}\right)\right], \text{and} \quad (10)$$

$$\bar{\eta}_{\mathrm{sum}} = \mathrm{E}\left[\sum_{i^*}\sum_{j^*\neq i^*}\log_2\left(1+\gamma_{i^*j^*,\mathrm{IBFD}}\right)\right], \quad (11)$$

where $\gamma_{i^*j^*,\mathrm{BC}}$, $\gamma_{i^*j^*,\mathrm{MAC}}$, $\gamma_{i^*j^*,K\text{-UserIC}}$, $\gamma_{i^*j^*,\mathrm{SDD}}$, and $\gamma_{i^*j^*,\mathrm{IBFD}}$ denote the effective signal-to-interference-plus-noise power ratio for the BC-based, MAC-based, K-UserIC-based, SDD-based, and IBFD-based schemes at the receiver, respectively, and are given by (12), (13), (14), (15), and (16) (see end of paper). ρ and ω denote the average signal to noise power ratio (SNR), which is defined as $\rho := P/\sigma^2$, and the average SI to noise power ratio (INR), which is defined as $\omega := \chi P/\sigma^2$, per antenna, respectively. Furthermore, Ω_{S}, $\Omega_{\mathrm{BC}}(j)$, $\Omega_{\mathrm{MAC}}(i)$, $\Omega_{\mathrm{CC}}(i,j)$, and $\Omega_{\mathrm{self}}(j)$ are, respectively, defined as follows:

$$\Omega_{\mathrm{S}} := \mathbf{g}_{i^*j^*}\mathbf{H}_{i^*j^*}\mathbf{f}_{i^*j^*}, \quad (17)$$

$$\Omega_{\mathrm{BC}}(j) := \mathbf{g}_{i^*j^*}\mathbf{H}_{i^*j^*}\mathbf{f}_{i^*j}, \quad (18)$$

$$\Omega_{\mathrm{MAC}}(i) := \mathbf{g}_{i^*j^*}\mathbf{H}_{ij^*}\mathbf{f}_{ij^*}, \quad (19)$$

$$\Omega_{\mathrm{CC}}(i,j) := \mathbf{g}_{i^*j^*}\mathbf{H}_{ij^*}\mathbf{f}_{ij}, \text{and} \quad (20)$$

$$\Omega_{\text{self}}(j) := \mathbf{g}_{i^*j^*}\tilde{\mathbf{H}}_{j^*j^*}\mathbf{f}_{j^*j}. \quad (21)$$

3.2 | Mathematical motivation for closed-form expression

3.2.1 | Achievable ergodic rate

From Jensen's inequality, that is, for random variable X, if $f(x)$ is a convex function, then $\mathrm{E}[f(X)] \le f(\mathrm{E}[X])$, and the achievable ergodic rate is bounded as follows:

$$\log_2\left(1+\mathrm{E}\left[\left(\frac{P_S}{P_I+P_N}\right)^{-1}\right]^{-1}\right) \le \mathrm{E}\left[\log_2\left(1+\frac{P_S}{P_I+P_N}\right)\right] \le \log_2\left(1+\mathrm{E}\left[\frac{P_S}{P_I+P_N}\right]\right). \quad (22)$$

Furthermore, using the results of [22], for a large number of transmit and receive antennas, the lower and upper bounds of the achievable ergodic rate of (22) converge to the same value. Thus, the achievable ergodic sum rate approximates to

$$\mathrm{E}\left[\sum^{N}\log_2\left(1+\frac{P_S}{P_I+P_N}\right)\right] \approx N\log_2\left(1+\frac{\mathrm{E}[P_S]}{\mathrm{E}[P_I+P_N]}\right). \quad (23)$$

3.2.2 | Maximum singular value

Using the results of [23] and [24], the maximum singular value $\alpha_{ij,1}$ of $\mathbf{H}_{ij}$, which is an $M_R \times M_T$ matrix, where the entries are complex Gaussian random variables, is bounded by

$${\alpha_{ij,1}}^2 \le \left(\sqrt{\frac{M_R}{M_T}}+1\right)^2 M_T \text{ or } {\alpha_{ij,1}}^2 \le \left(\sqrt{\frac{M_T}{M_R}}+1\right)^2 M_R, \quad (24)$$

and asymptotically approaches the bound for a large number of M_T or M_R. Thus, the expectation of the maximum singular value ${\alpha_{ij,1}}^2$ approximates to

$$\mathrm{E}\left[{\alpha_{ij,1}}^2\right] \approx \left(\sqrt{M_T}+\sqrt{M_R}\right)^2. \quad (25)$$

The authors of [24] propose $M_R \cdot M_T$ larger than 250 as the large number.

3.2.3 | Expectation of interference power

Let $v_{ij,k}(m)$, $u_{ij,k}(m)$, $f_{ij}(m)$, and $g_{ij}(m)$ be the m-th entries of $\mathbf{v}_{ij,k}$, $\mathbf{u}_{ij,k}$, $\mathbf{f}_{ij}$, and $\mathbf{g}_{ij}$, respectively, where $k = 1, 2, \dots, M_{\min}$, and $M_{\min}$ denotes the minimum value between M_T and M_R. Furthermore, for $v_{ij,k}(m)$ and $f_{ij}(m)$, $m = 1, 2, \dots, M_T$, and for $u_{ij,k}(m)$ and $g_{ij}(m)$, $m = 1, 2, \dots, M_R$.

For any k, $v_{ij,k}(m)$, $u_{ij,k}(m)$, $f_{ij}(m)$, and $g_{ij}(m)$ satisfy $\Sigma_m|v_{ij,k}(m)|^2 = 1$, $\Sigma_m|u_{ij,k}(m)|^2 = 1$, $\Sigma_m|f_{ij}(m)|^2 = 1$, and $\Sigma_m|g_{ij}(m)|^2 = 1$, respectively, because $\mathbf{v}_{ij,k}$ and $\mathbf{u}_{ij,k}$ are singular vectors. Furthermore, $v_{ij,k}(m)$, $u_{ij,k}(m)$, $f_{ij}(m)$, and $g_{ij}(m)$ also satisfy $\mathrm{E}[|v_{ij,k}(m)|^2] = 1/M_T$, $\mathrm{E}[|u_{ij,k}(m)|^2] = 1/M_R$, $\mathrm{E}[|f_{ij}(m)|^2] = 1/M_T$, and $\mathrm{E}[|g_{ij}(m)|^2] = 1/M_R$, respectively, because $v_{ij,k}(m)$, $u_{ij,k}(m)$, $f_{ij}(m)$, and $g_{ij}(m)$ have the same probability distribution, and are independent of each other. Thus, the expectation of the BC interference power is obtained by

$$\begin{aligned}
&\mathrm{E}\left[\left|\mathbf{g}_{i^*j^*}\mathbf{H}_{i^*j^*}\mathbf{f}_{i^*j}\right|^2\right] = \mathrm{E}\left[\left|\alpha_{i^*j^*,1}\mathbf{v}_{i^*j^*,1}{}^{\mathrm{H}}\mathbf{f}_{i^*j}\right|^2\right] \\
&= \mathrm{E}\left[\left|\alpha_{i^*j^*,1}\right|^2\right]\mathrm{E}\left[\left|\textstyle\sum_{m=1}^{M_T} v_{i^*j^*,1}(m)f_{i^*j}(m)\right|^2\right] \\
&= \mathrm{E}\left[\left|\alpha_{i^*j^*,1}\right|^2\right]\mathrm{E}\left[\textstyle\sum_{m=1}^{M_T}\left|v_{i^*j^*,1}(m)\right|^2\left|f_{i^*j}(m)\right|^2\right] \\
&= \mathrm{E}\left[\left|\alpha_{i^*j^*,1}\right|^2\right]M_T\mathrm{E}\left[\left|v_{i^*j^*,1}(m)\right|^2\right]\mathrm{E}\left[\left|f_{i^*j}(m)\right|^2\right] \\
&\approx \left(\sqrt{M_T}+\sqrt{M_R}\right)^2\frac{M_T}{{M_T}^2} = \left(1+\sqrt{\frac{M_R}{M_T}}\right)^2.
\end{aligned} \quad (26)$$

Similarly, the expectation of the MAC interference power is obtained by

$$\mathrm{E}\left[\left|\mathbf{g}_{i^*j^*}\mathbf{H}_{ij^*}\mathbf{f}_{ij^*}\right|^2\right] \approx \left(\sqrt{\frac{M_T}{M_R}}+1\right)^2. \quad (27)$$

Furthermore, using $\Sigma_k\mathrm{E}[|\alpha_{ij,k}|^2] = M_T M_R$ because the summation of the expectation of all squared singular values is equal to the product of the number of transmit and receive antennas, the expectation of the co-channel interference power is obtained by

$$\begin{aligned}
&\mathrm{E}\left[\left|\mathbf{g}_{i^*j^*}\mathbf{H}_{ij^*}\mathbf{f}_{ij}\right|^2\right] = \mathrm{E}\left[\left|\mathbf{g}_{i^*j^*}\mathbf{U}_{ij^*}\mathbf{\Sigma}_{ij^*}\mathbf{V}_{ij^*}{}^{\mathrm{H}}\mathbf{f}_{ij}\right|^2\right] \\
&= \mathrm{E}\left[\left|\textstyle\sum_{k=1}^{M_{\min}}\mathbf{g}_{i^*j^*}\mathbf{u}_{ij^*,k}\alpha_{ij^*,k}\mathbf{v}_{ij^*,k}{}^{\mathrm{H}}\mathbf{f}_{ij}\right|^2\right] \\
&= \mathrm{E}\left[\left|\textstyle\sum_{k=1}^{M_{\min}}\left(\alpha_{ij^*,k}\sum_{m=1}^{M_R} g_{i^*j^*}(m)u_{ij^*,k}(m)\right.\right.\right. \\
&\qquad\left.\left.\left.\cdot\textstyle\sum_{m=1}^{M_T} v_{ij^*,k}(m)f_{ij}(m)\right)\right|^2\right] \\
&= \textstyle\sum_{k=1}^{M_{\min}}\left(\mathrm{E}\left[\left|\alpha_{ij^*,k}\right|^2\right]\mathrm{E}\left[\sum_{m=1}^{M_R}\left|g_{i^*j^*}(m)u_{ij^*,k}(m)\right|^2\right]\right. \\
&\qquad\left.\cdot\mathrm{E}\left[\sum_{m=1}^{M_T}\left|v_{ij^*,k}(m)f_{ij}(m)\right|^2\right]\right) \\
&= \textstyle\sum_{k=1}^{M_{\min}}\left(\mathrm{E}\left[\left|\alpha_{ij^*,k}\right|^2\right]\right)\frac{M_R}{{M_R}^2}\frac{M_T}{{M_T}^2} \\
&= M_T M_R\frac{M_R}{{M_R}^2}\frac{M_T}{{M_T}^2} = 1.
\end{aligned} \quad (28)$$

Similarly, the expectation of the SI power is obtained by

$$\mathrm{E}\left[\left|\mathbf{g}_{i^*j^*}\tilde{\mathbf{H}}_{j^*j^*}\mathbf{f}_{j^*j}\right|^2\right] = 1. \quad (29)$$

3.3 | Closed-form expression of achievable ergodic sum rate

For a large number of antennas, using the approximation of the achievable ergodic sum rate from (23), the approximation of the maximum singular value from (25), the derivation and approximation of the interference power from (26), (27), (28), and (29), the closed-form expressions of the achievable ergodic sum rate for the BC-based, MAC-based, K-UserIC-based, SDD-based, and IBFD-based schemes are

given by (30), (31), (32), (33), and (34) (see the last page), respectively. Note that $E[|S_R(i^*)|/|S_R(i)|] = 1$, $E[|S_R(i^*)|/|S_R(j)|] = 1$, and $E[|S_R(i^*)|] = 1/2$ because for the SDD-based scheme, we consider a randomly selected link direction between a pair of nodes, as explained in Section 2.1.

4 | NUMERICAL RESULTS

In this section, we present the numerical evaluation results of the achievable ergodic sum rate for each transmission scheme to support fully connected links among N nodes. This was obtained using Monte Carlo simulation, averaging the achievable sum rate for the randomly generated channel for 1,000 trials. Furthermore, we compared the results using closed-form expressions. Note that we assume that $\omega = 0$ dB. This means that SI has been removed to a level that is similar to the thermal noise. In Figures 4 and 5, the results are, respectively, displayed for $N = 4$ and $N = 16$ with $M_T = M_R = 64$. In Figures 6 and 7, the results are, respectively, displayed for $N = 4$ and $N = 16$ with $M_T = M_R = 256$.

Let X and Y be independent random variables, and let c be a constant value. For a high-SNR region and a small N, the achievable ergodic sum rate and closed-form expression can be simplified as $E[\log_2(1 + c/X)]$ and $\log_2(1 + c/E[X])$, respectively, because the expectation of the numerator is considerably larger than that of the denominator. Thus, the achievable ergodic sum rate is greater than the closed-form expression, as observed in Figures 4 and 6, because $E[\log_2(1 + c/X)] \geq \log_2(1 + c/E[X])$. For a high-SNR region and a large N, the achievable ergodic sum rate and closed-form expression can be simplified as $E[\log_2(1 + Y/X)]$ and $\log_2(1 + E[Y/X])$, respectively. Thus, the achievable ergodic sum rate is less than the closed-form expression, as observed in Figures 5 and 7, because $E[\log_2(1 + Y/X)] \leq \log_2(1 + E[Y/X])$. However, the closed-form expression is more accurate for a large number of M_T and M_R compared to N, and there is a small difference between the achievable ergodic sum rate and he closed-form expression for a low-SNR region.

For the high-SNR region, the acceptable performance was demonstrated in the order IBFD-based scheme, SDD-based scheme, K-UserIC-based scheme, and BC/MAC-based schemes. The BC-based scheme and MAC-based scheme demonstrated virtually the same performance for the high-SNR region. For the low-SNR region, the MAC-

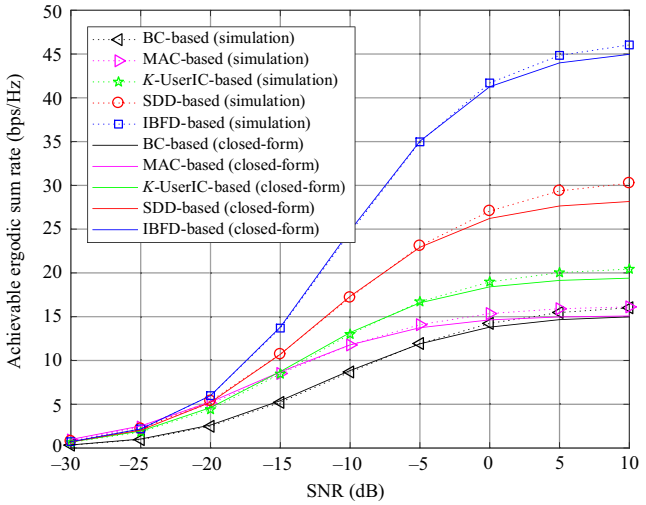

FIGURE 4 SNR vs achievable ergodic sum rate: simulations (markers) and closed-form expressions (solid lines) for $N = 4$, $M_T = 64$, $M_R = 64$, and $\omega = 0$ dB

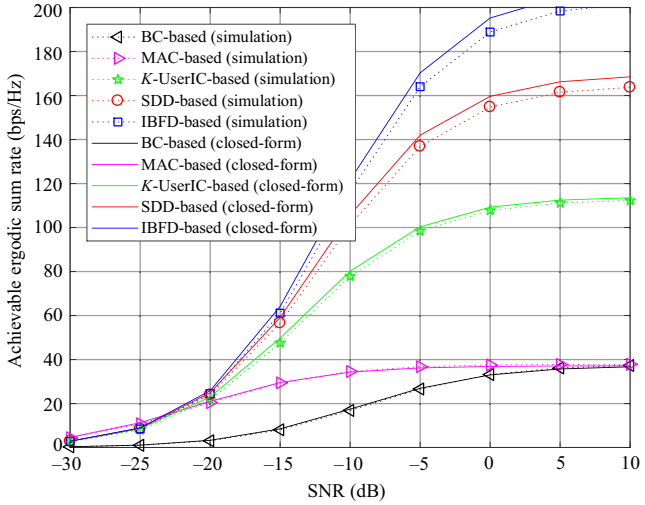

FIGURE 5 SNR vs achievable ergodic sum rate: simulations (markers) and closed-form expressions (solid lines) for $N = 16$, $M_T = 64$, $M_R = 64$, and $\omega = 0$ dB

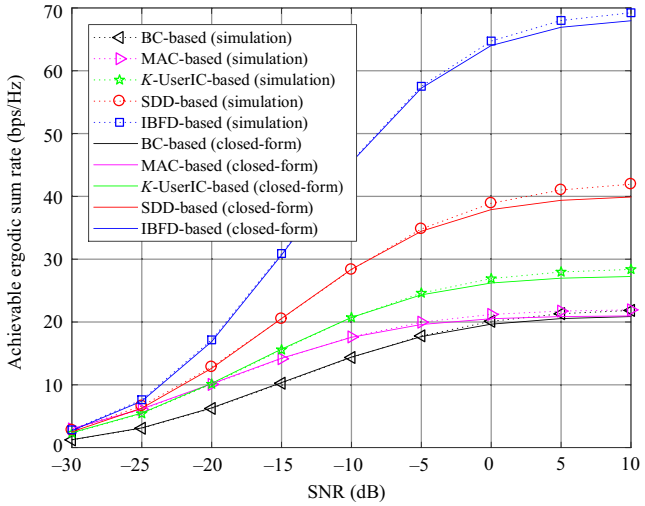

FIGURE 6 SNR vs achievable ergodic sum rate: simulations (markers) and closed-form expressions (solid lines) for $N = 4$, $M_T = 256$, $M_R = 256$, and $\omega = 0$ dB

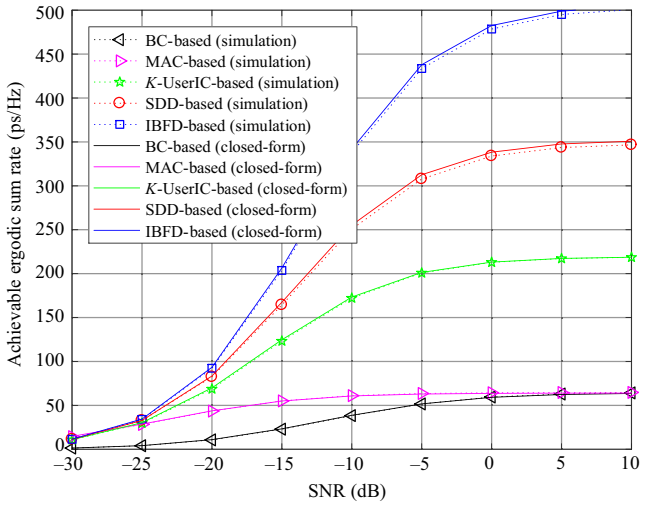

FIGURE 7 SNR vs achievable ergodic sum rate: simulations (markers) and closed-form expressions (solid lines) for $N = 16$, $M_T = 256$, $M_R = 256$, and $\omega = 0$ dB

based scheme demonstrated the best performance because the transmit power of each node is limited by P; however, there was only a small difference for the BC-based scheme. For the low-SNR region, there was a minimal performance gap between the IBFD-based scheme and SDD-based scheme; however, even for the high-SNR region, the performance gap decreased for a larger N. Furthermore, although we assumed that SI was removed to a level similar to the thermal noise, the performance degradation resulting from a shortage of SIC was more severe in the IBFD-based scheme. Thus, the performance improvements of the IBFD-based scheme compared to the SDD-based scheme may not be as high as expected.

5 | CONCLUSION

In this paper, we investigated transmission schemes to support fully connected N nodes for HD and FD, analyzed the achievable ergodic sum rate among N nodes, and proposed a closed-form expression of the achievable ergodic sum rate for each scheme.

We confirmed that the closed-form expression is almost as accurate for a large number of M_T and M_R when compared to N. Furthermore, we compared the performance for each scheme. For a high-SNR region, an acceptable performance was demonstrated in the order IBFD-based scheme, SDD-based scheme, K-UserIC-based scheme, and BC/MAC-based schemes. For a low-SNR region, the MAC-based scheme demonstrated the best performance. Compared to the SDD-based scheme, the performance improvements of the IBFD-based scheme may not be as high as expected according to the SIC performance.

ACKNOWLEDGMENTS

This work was supported by the Institute for Information & Communications Technology Promotion (IITP) grant funded by the Korea government (MSIT) (No. 2014-0-00282, Development of 5G Mobile Communication Technologies for Hyper-connected Smart Services).

REFERENCES

1. ITU-R SG05 Contribution 40, *Minimum requirements related to technical performance for IMT-2020 radio interface(s)*, Feb. 23, 2017.
2. NGMN Alliance, *NGMN 5G White Paper*, Feb. 17, 2015.
3. F. Boccardi et al., *Five disruptive technology directions for 5G*, IEEE Commun. Mag. **52** (2014), no. 2, 74–80.
4. R. J. Weiler et al., Enabling 5G backhaul and access with millimeter-waves, *Eur. Conf. Netw. Commun.*, Bologna, Italy, June 23–26, 2014, pp. 1–5.
5. E. G. Larsson et al., *Massive MIMO for next generation wireless systems*, IEEE Commun. Mag. **52** (2014), no. 2, 186–195.
6. Z. Zhang et al., *Large-scale MIMO-based wireless backhaul in 5G networks*, IEEE Wireless Commun. **22** (2015), no. 5, 58–66.
7. H. S. Dhillon and G. Caire, *Wireless backhaul networks capacity bound, scalability analysis and design guidelines*, IEEE Trans. Wireless Commun. **14** (2015), no. 11, 6043–6056.
8. W. Feng et al., *Millimetre-wave backhaul for 5G networks challenges and solutions*, Sens. **16** (2016), no. 6, 892:1–892:17.
9. H. Abbas, K. Hamdi, and Full duplex relay in millimeter wave backhaul links, *IEEE Conf. Wireless Commun. Netw. Conf.*, Doha, Qatar, Apr. 3–6, 2016, pp. 1–6.
10. A. Sharma, R. K. Ganti, and J. K. Milleth, *Joint backhaul-access analysis of full duplex elf-backhauling heterogeneous networks*, IEEE Trans. Wirel. Commun. **16** (2017), no. 3, 1727–1740.
11. S. Rajagopal, R. Taori, and S. Abu-Surra, Self-interference mitigation for in-band mmWave wireless backhaul, *Consumer Commun. Netw. Conf.*, Las Vegas, USA, Jan. 10–13, 2014, pp. 551–556.
12. A. I. Nasr and Y. Fahmy, Millimeter-wave wireless backhauling for 5G small cells: Star versus mesh topologies, *Int. Conf. Microelectron.*, Giza, Egypt, Dec. 17–20, 2016, pp. 85–88.
13. T. L. Marzetta, *Noncooperative cellular wireless with unlimited numbers of base station antennas*, IEEE Trans. Wireless Commun. **9** (2010), no. 11, 3590–3600.
14. H. Q. Ngo, E. G. Larsson, and T. L. Marzetta, *Energy and spectral efficiency of very large multiuser MIMO system*, IEEE Trans. Commun. **61** (2013), no. 4, 1436–1449.
15. F. Rusek et al., *Scaling up MIMO: Opportunities and challenges with large arrays*, IEEE Signal Process. Mag. **30** (2013), no. 1, 40–60.
16. A. Sabharwal et al., *In-band full-duplex wireless: Challenges and opportunities*, IEEE J. Sel. Areas Commun. **32** (2014), no. 9, 1637–1652.
17. E. Everett, A. Sahai, and A. Sabharwal, *Passive self-interference suppression for full-duplex infrastructure nodes*, IEEE Trans. Wireless Commun. **13** (2004), no. 2, 680–694.
18. B. Yin et al., Full-duplex in large-scale wireless systems, *Asilomar Conf. Signals, Syst. Comput.*, Pacific Grove, USA, Nov. 3–6, 2013, pp. 1623–1627.

19. C. Wang et al., *On the performance of the MIMO zero-forcing receiver in the presence of channel estimation error*, IEEE Trans. Wireless Commun. **6** (2007), no. 3, 805–810.
20. Y. Wang and S. Mao, *On distributed power control in full duplex wireless networks*, Digital Commun. Netw. **3** (2017), no. 1, 1–10.
21. W. Cheng, X. Zhang, and H. Zhang, Optimal dynamic power control for full-duplex bidirectional-channel based wireless networks, *IEEE Int. Conf. Comput. Commun.*, Turin, Italy, Apr. 14–19, 2013, pp. 3120–3128.
22. Y. Lim, C. Chae, and G. Caire, *Performance analysis of massive MIMO for cell-boundary users*, IEEE Trans. Wireless Commun. **14** (2015), no. 12, 6827–6842.
23. J. B. Andersen, *Array gain and capacity for known random channels with multiple element arrays at both ends*, IEEE J. Sel. Areas Commun. **18** (2000), no. 11, 2172–2178.
24. T. Taniguchi, S. Sha, and Y. Karasawa, An approximation of eigenvalue distribution in i.i.d MIMO channels under Rayleigh fading, *IEEE/SP Workshop Stat. Signal Process.*, Bordeaux, France, July 17–20, 2005, pp. 1072–1077.

AUTHOR BIOGRAPHIES

Seokki Kim received his BS and MS degrees in electrical and electronics engineering at the Chung-Ang University, Seoul, Rep. of Korea, in 2007 and 2009, respectively. Since 2009, he has been with the Future Mobile Communication Research Division at the Electronics and Telecommunications Research Institute, Daejeon, Rep. of Korea, where he is now a senior researcher. His main research interests are 5G and beyond 5G mobile communications.

Seungkwon Baek received his MS degree in computer engineering from the Kyungpook National University, Daeju, Rep. of Korea, in 2000. From 2000, he was a principle researcher at the Electronics and Telecommunications Research Institute, Daejeon, Rep. of Korea, where he worked on RAN architecture and protocol engineering for mobile communication systems. He is now a project leader in the Future Mobile Communication Research Division in the Hyper-connected Communication Research Laboratory. His research interests include network architecture and radio access for mobile communications, with a focus on mobility control and radio-resource management.

$$\mathbf{y}_{j^*} = \underbrace{\sqrt{\tfrac{P}{N-1}}\mathbf{H}_{i^*j^*}\mathbf{f}_{i^*j^*}\mathbf{x}_{i^*j^*}}_{\text{Desired signal}} + \underbrace{\textstyle\sum_{j\neq i^*,j^*}\sqrt{\tfrac{P}{N-1}}\mathbf{H}_{i^*j^*}\mathbf{f}_{i^*j}\mathbf{x}_{i^*j}}_{\text{Broadcast channel interference}} + \mathbf{n}_{j^*}. \tag{1}$$

$$\mathbf{y}_{j^*} = \underbrace{\sqrt{P}\mathbf{H}_{i^*j^*}\mathbf{f}_{i^*j^*}\mathbf{x}_{i^*j^*}}_{\text{Desired signal}} + \underbrace{\textstyle\sum_{i\neq i^*,j^*}\sqrt{P}\mathbf{H}_{ij^*}\mathbf{f}_{ij^*}\mathbf{x}_{ij^*}}_{\text{Multiple access channel interference}} + \mathbf{n}_{j^*}. \tag{2}$$

$$\mathbf{y}_{j^*} = \underbrace{\sqrt{\tfrac{P}{N-K}}\mathbf{H}_{i^*j^*}\mathbf{f}_{i^*j^*}\mathbf{x}_{i^*j^*}}_{\text{Desired signal}} + \underbrace{\textstyle\sum_{\substack{j>K\\ j\neq j^*}}\sqrt{\tfrac{P}{N-K}}\mathbf{H}_{i^*j^*}\mathbf{f}_{i^*j}\mathbf{x}_{i^*j}}_{\text{Broadcast channel interference}} + \underbrace{\textstyle\sum_{\substack{i\leq K\\ i\neq i^*}}\sqrt{\tfrac{P}{N-K}}\mathbf{H}_{ij^*}\mathbf{f}_{ij^*}\mathbf{x}_{ij^*}}_{\text{Multiple access channel interference}} + \underbrace{\textstyle\sum_{\substack{i\leq K\\ i\neq i^*}}\sum_{\substack{j>K\\ j\neq j^*}}\sqrt{\tfrac{P}{N-K}}\mathbf{H}_{ij^*}\mathbf{f}_{ij}\mathbf{x}_{ij}}_{\text{Co-channel interference}} + \mathbf{n}_{j^*}. \tag{3}$$

$$\begin{aligned}\mathbf{y}_{j^*} = {} & \underbrace{\sqrt{\tfrac{P}{|S_{\mathrm{R}}(i^*)|}}\mathbf{H}_{i^*j^*}\mathbf{f}_{i^*j^*}\mathbf{x}_{i^*j^*}}_{\text{Desired signal}} + \underbrace{\textstyle\sum_{j\in S_{\mathrm{R}}(i^*),\, j\neq j^*}\sqrt{\tfrac{P}{|S_{\mathrm{R}}(i^*)|}}\mathbf{H}_{i^*j^*}\mathbf{f}_{i^*j}\mathbf{x}_{i^*j}}_{\text{Broadcast channel interference}} + \underbrace{\textstyle\sum_{i\in S_{\mathrm{T}}(j^*),\, i\neq i^*}\sqrt{\tfrac{P}{|S_{\mathrm{R}}(i)|}}\mathbf{H}_{ij^*}\mathbf{f}_{ij^*}\mathbf{x}_{ij^*}}_{\text{Multiple access channel interference}} \\ & + \underbrace{\textstyle\sum_{i\neq i^*,j^*}\sum_{j\in S_{\mathrm{R}}(i),\, j\neq j^*}\sqrt{\tfrac{P}{|S_{\mathrm{R}}(i)|}}\mathbf{H}_{ij^*}\mathbf{f}_{ij}\mathbf{x}_{ij}}_{\text{Co-channel interference}} + \underbrace{\textstyle\sum_{j\in S_{\mathrm{R}}(j^*)}\sqrt{\tfrac{P}{|S_{\mathrm{R}}(j^*)|}}\tilde{\mathbf{H}}_{j^*j^*}\mathbf{f}_{j^*j}\mathbf{x}_{j^*j}}_{\text{Self-interference}} + \mathbf{n}_{j^*}.\end{aligned} \tag{4}$$

$$\begin{aligned}\mathbf{y}_{j^*} = {} & \underbrace{\sqrt{\tfrac{P}{N-1}}\mathbf{H}_{i^*j^*}\mathbf{f}_{i^*j^*}\mathbf{x}_{i^*j^*}}_{\text{Desired signal}} + \underbrace{\textstyle\sum_{j\neq i^*,j^*}\sqrt{\tfrac{P}{N-1}}\mathbf{H}_{i^*j^*}\mathbf{f}_{i^*j}\mathbf{x}_{i^*j}}_{\text{Broadcast channel interference}} + \underbrace{\textstyle\sum_{i\neq i^*,j^*}\sqrt{\tfrac{P}{N-1}}\mathbf{H}_{ij^*}\mathbf{f}_{ij^*}\mathbf{x}_{ij^*}}_{\text{Multiple access channel interference}} \\ & + \underbrace{\textstyle\sum_{i\neq i^*,j^*}\sum_{j\neq i,j^*}\sqrt{\tfrac{P}{N-1}}\mathbf{H}_{ij^*}\mathbf{f}_{ij}\mathbf{x}_{ij}}_{\text{Co-channel interference}} + \underbrace{\textstyle\sum_{j\neq j^*}\sqrt{\tfrac{P}{N-1}}\tilde{\mathbf{H}}_{j^*j^*}\mathbf{f}_{j^*j}\mathbf{x}_{j^*j}}_{\text{Self-interference}} + \mathbf{n}_{j^*}.\end{aligned} \tag{5}$$

$$\gamma_{i^*j^*,\mathrm{BC}} = \frac{|\Omega_{\mathrm{S}}|^2}{\sum_{j\neq i^*,j^*}|\Omega_{\mathrm{BC}}(j)|^2 + \frac{N-1}{\rho}}. \tag{12}$$

$$\gamma_{i^*j^*,\mathrm{MAC}} = \frac{|\Omega_{\mathrm{S}}|^2}{\sum_{i\neq i^*,j^*}|\Omega_{\mathrm{MAC}}(i)|^2 + \frac{1}{\rho}}. \tag{13}$$

$$\gamma_{i^*j^*,K\text{-UserIC}} = \frac{|\Omega_{\mathrm{S}}|^2}{\sum_{\substack{j>K\\ j\neq j^*}}|\Omega_{\mathrm{BC}}(j)|^2 + \sum_{\substack{i\leq K\\ i\neq i^*}}|\Omega_{\mathrm{MAC}}(i)|^2 + \sum_{\substack{i\leq K\\ i\neq i^*}}\sum_{\substack{j>K\\ j\neq j^*}}|\Omega_{\mathrm{CC}}(i,j)|^2 + \frac{N-K}{\rho}}. \tag{14}$$

$$\gamma_{i^*j^*,\mathrm{SDD}} = \frac{|\Omega_{\mathrm{S}}|^2}{\sum_{j\in S_{\mathrm{R}}(i^*),\, j\neq j^*}\frac{|S_{\mathrm{R}}(i^*)|}{|S_{\mathrm{R}}(i^*)|}|\Omega_{\mathrm{BC}}(j)|^2 + \sum_{i\in S_{\mathrm{T}}(j^*),\, i\neq i^*}\frac{|S_{\mathrm{R}}(i^*)|}{|S_{\mathrm{R}}(i)|}|\Omega_{\mathrm{MAC}}(i)|^2 + \sum_{i\neq i^*,j^*}\sum_{j\in S_{\mathrm{R}}(i),\, j\neq j^*}\frac{|S_{\mathrm{R}}(i^*)|}{|S_{\mathrm{R}}(i)|}|\Omega_{\mathrm{CC}}(i,j)|^2 + \frac{\omega}{\rho}\sum_{j\in S_{\mathrm{R}}(j^*)}\frac{|S_{\mathrm{R}}(i^*)|}{|S_{\mathrm{R}}(j^*)|}|\Omega_{\mathrm{self}}(j)|^2 + \frac{|S_{\mathrm{R}}(i^*)|}{\rho}}. \tag{15}$$

$$\gamma_{i^*j^*,\mathrm{IBFD}} = \frac{|\Omega_{\mathrm{S}}|^2}{\sum_{j\neq i^*,j^*}|\Omega_{\mathrm{BC}}(j)|^2 + \sum_{i\neq i^*,j^*}|\Omega_{\mathrm{MAC}}(i)|^2 + \sum_{i\neq i^*,j^*}\sum_{j\neq i,j^*}|\Omega_{\mathrm{CC}}(i,j)|^2 + \frac{\omega}{\rho}\sum_{j\neq j^*}|\Omega_{\mathrm{self}}(j)|^2 + \frac{N-1}{\rho}}. \tag{16}$$

$$\bar{\eta}_{\mathrm{sum}} \approx (N-1)\log_2\left(1 + \frac{\left(\sqrt{M_{\mathrm{T}}} + \sqrt{M_{\mathrm{R}}}\right)^2}{(N-2)\left(1+\sqrt{\frac{M_{\mathrm{R}}}{M_{\mathrm{T}}}}\right)^2 + \frac{N-1}{\rho}}\right). \tag{30}$$

$$\bar{\eta}_{\mathrm{sum}} \approx (N-1)\log_2\left(1 + \frac{\left(\sqrt{N_{\mathrm{T}}} + \sqrt{N_{\mathrm{R}}}\right)^2}{(N-2)\left(\sqrt{\frac{M_{\mathrm{T}}}{M_{\mathrm{R}}}}+1\right)^2 + \frac{1}{\rho}}\right). \tag{31}$$

$$\bar{\eta}_{\mathrm{sum}} \approx \left\lceil\frac{N}{2}\right\rceil \cdot \left\lfloor\frac{N}{2}\right\rfloor \log_2\left(1 + \frac{\left(\sqrt{M_{\mathrm{T}}} + \sqrt{M_{\mathrm{R}}}\right)^2}{\frac{N-2}{2}\left(1+\sqrt{\frac{M_{\mathrm{R}}}{M_{\mathrm{T}}}}\right)^2 + \frac{N-2}{2}\left(\sqrt{\frac{M_{\mathrm{T}}}{M_{\mathrm{R}}}}+1\right)^2 + \left\lceil\frac{N-2}{2}\right\rceil \cdot \left\lfloor\frac{N-2}{2}\right\rfloor + \frac{N}{2\rho}}\right). \tag{32}$$

$$\bar{\eta}_{\mathrm{sum}} \approx {}_N\mathrm{C}_2\log_2\left(1 + \frac{\left(\sqrt{M_{\mathrm{T}}} + \sqrt{M_{\mathrm{R}}}\right)^2}{\frac{N-2}{2}\left(1+\sqrt{\frac{M_{\mathrm{R}}}{M_{\mathrm{T}}}}\right)^2 + \frac{N-2}{2}\left(\sqrt{\frac{M_{\mathrm{T}}}{M_{\mathrm{R}}}}+1\right)^2 + \frac{(N-2)^2}{2} + \frac{(N-2)\omega}{2\rho} + \frac{N}{2\rho}}\right). \tag{33}$$

$$\bar{\eta}_{\mathrm{sum}} \approx 2{}_N\mathrm{C}_2\log_2\left(1 + \frac{\left(\sqrt{M_{\mathrm{T}}} + \sqrt{M_{\mathrm{R}}}\right)^2}{(N-2)\left(1+\sqrt{\frac{M_{\mathrm{R}}}{M_{\mathrm{T}}}}\right)^2 + (N-2)\left(\sqrt{\frac{M_{\mathrm{T}}}{M_{\mathrm{R}}}}+1\right)^2 + (N-2)^2 + (N-1)\frac{\omega}{\rho} + \frac{N-1}{\rho}}\right). \tag{34}$$